Electronic Supplementary Material (ESI) for Materials Horizons.
This journal is © The Royal Society of Chemistry 2021

Methods, supplementary figures and tables

Super-ions of sodium cations with hydrated hydroxide anions: inorganic structure-directing agents in zeolite synthesis

Karel Asselman[†a], Nick Pellens[†a], Sambhu Radhakrishnan[a,b], C. Vinod Chandran[a,b], Johan Martens[a,b], Francis Taulelle[a,b], Toon Verstraelen[c], Matti Hellström[d], Eric Breynaert[*,a,b], Christine E.A. Kirschhock[a]

Contents

1. Methods

1.1. Sample preparation

Zeolite samples are synthesized using the reported method via hydrated silicate ionic liquids (HSILs)[1]. HSILs are prepared by mixing TEOS (Acros Organics, 98%),NaOH (Fischer Scientific, 98+%) and milliQ H_2O), into an emulsion with molar ratios 1 TEOS : 1.5 NaOH: 25 H_2O under continuous stirring. After complete

hydrolysis of TEOS into silicic acid and ethanol, spontaneous liquid-liquid phase separation results in an upper water-ethanol phase, and a dense HSIL phase with final composition 1 SiO_2 : 1.5 NaOH : 4.31 H_2O, as determined via gravimetric analysis, which is collected using a separation funnel. To achieve the desired compositions for zeolite synthesis, the HSIL is combined with $Al(OH)_3$ hydrate powder (Sigma Aldrich), NaOH pellets (Fischer Scientific) and H_2O. The mixtures are aged overnight under continuous stirring, transferred to PP vessels and crystallized in a tumbling oven at 60°C for 7 days. Higher synthesis temperatures for sodalite samples were observed to increase overall crystallinity and crystal size. One synthesis was therefore performed at a temperature of 170°C for 2 days, with batch composition 0.5 SiO_2 : 0.013 Al_2O_3 : 2.5 NaOH : 7.5 H_2O. This produced high quality, clean faceted, micron-sized crystals and served as the reference sample and starting structure for refinement of other samples crystallized at 60°C. Samples were separated from the mother liquor by centrifugation and washed by Buchner filtration with moderate amounts of water to avoid extraction of NaOH included in the pores of hydroxysodalite samples. The solids were subsequently dried at 60°C and later stored at ambient conditions prior to further characterization. Samples are labelled according to the cation hydration [H_2O]/[NaOH] value and batch alkalinity [Si]/[NaOH] of the synthesis mixture (ESI table 1). For example, the label SOD 7–0.1 indicates a hydroxysodalite synthesized from a synthesis mixture with cation hydration and alkalinity of 7 and 0.1, respectively.

1.2. Characterization

High-resolution scanning electron microscopy (SEM) images are recorded with a Nova NanoSEM450 (FEI, Hillsboro, OR). For chemical analysis, Si and Al contents are determined on an axial simultaneous ICP-OES instrument (Varian 720-ES) with cooled cone interface and oxygen-free optics. Samples for ICP were prepared by digesting 50 mg of zeolite powder with 250 mg $LiBO_2$ in a muffle furnace at 1000°C prior to diluting with 0.42N HNO_3 solution. Thermogravimetric analysis (TGA) is performed on a TGA Q500 (TA instruments) under N_2 flow (10 ml/min) with a heating rate of 2°C/min between

room temperature and 750°C. Samples were kept at a constant temperature of 60°C for 120mins before further heating to remove physisorbed water. Fourier transform infrared (FT-IR) measurements were performed at room temperature using the KBr pellet technique on a Bruker IFS 66v/S spectrometer in transmission mode.

1.3. XRD analysis

Laboratory high-throughput PXRD patterns are recorded at room temperature on a STOE STADI P Combi diffractometer (CuKα_1 radiation), with focusing Ge(111) monochromator and a 140° curved image plate position sensitive detector. Laboratory high-resolution PXRD pattern for refinement were recorded on a STOE STADI MP diffractometer (CuKα_1 radiation), with focusing Ge(111) monochromator in Debye-Scherrer geometry (capillary Ø0.5mm), with a linear position sensitive detector (internal resolution 0.1°) at room temperature.

Explicit structures were derived for samples *SOD 3–0.2*, *SOD 7-0.1 and SOD 4.5-0.2* using an NMR-crystallography approach:

Rietveld refinement of the respective high resolution XRD-patterns is performed with the GSAS package[2]. Structure refinement started on sample *SOD 3–0.2*, leading to starting parameters for all Rietveld refinements. Structure refinement occurred in the cubic space group P$\bar{4}$3n with lattice constant 8.888 Å. The starting coordinates for the framework and sodium atoms were taken from literature[3]. One oxygen site, representative for water and hydroxyl molecules, was added on a general position after inspecting the difference Fourier map. Due to the limited number of scatterers, all positional parameters, occupancies and thermal displacement factors could be refined simultaneously without the need for soft restraints on bond lengths and angles. Only the occupancy factors of framework atoms were fixed at 1. The refinement readily converged with agreement factor R_{wp} of 6.5%. The T-O bond lengths for Si and Al are 1.6001(12), 1.7472(12), near their ideal values, indicating the ordered and highly crystalline nature of the

material. Comparison with NMR revealed notable presence of a second cage decoration in this sample (*SOD 3–0.2*), with a ratio of different sodium coordinations of 3:1. Closer inspection of the difference Fourier maps revealed high anisotropy of the earlier determined oxygen position in the cages and a split position was assumed, which led to two oxygen sites (OZ and OEZ) in accordance with the NMR observation. Concise analysis of the NMR data and periodic density functional theory (DFT) simulation revealed this oxygen position to be associated to cages containing 2 water molecules, one hydroxide anion and 4 sodium ions (EZ: extended Zundel ion). The oxygen site deduced by XRD is in excellent agreement with the structure derived by DFT and consistent with the NMR results.

Next the samples *SOD 7-0.1 and SOD 4.5-0.2* were analysed. Both showed spurious reflections, which could not be associated to any zeolite phase but rather arose from the very gentle sample preparation to avoid any leaching of NaOH from the samples. Samples were only rinsed once after centrifugation. Therefore, mother liquor rich in silicate and NaOH remained on the crystallites' surface. The residue can be removed by more extensive washing and most probably consists of sodium silicate and/or sodium hydroxide. The related intensities are very low and well separated from the SOD reflections. Even in the case of some overlap with the SOD peaks, the observed intensities would barely change. The observation that spurious H or Na signals do not show up in the NMR spectra confirms their minor presence, and we are confident in the validity of the diffraction analysis due to the excellent correspondence with the NMR quantification (vide infra).

In the *SOD 3–0.2* sample neither NMR, nor XRD revealed clear presence of cages containing only water next to 3 sodium ions. However, in the two samples synthesized at 60°C (*SOD 7-0.1 and SOD 4.5-0.2)* a ^{23}Na NMR signal in accordance with the work of Engelhard et al. associated to cages without hydroxide anion and with only 3 sodium ions was observed. Using fixed positions for oxygen atoms related to Zundel (Z) and Extended Zundel (EZ) anions and with occupation numbers derived

by NMR, the electron density maps of the samples were inspected and indeed a site in accordance with literature was identified for water molecules associated to cages containing only water (Water cages), linking the three sodium cations in edge sharing octahedral coordination.

Finally, Rietveld refinement of all three samples (*SOD 3–0.2*, *SOD 7-0.1 and SOD 4.5-0.2*), using all three types of oxygen (OZ,OEZ, OW) was performed with fixed oxygen sites and variable occupation numbers, also for sodium. The obtained results are listed together with the corresponding refined diffractograms in section 2.2 and are in excellent agreement with NMR results and DFT simulations.

From the refined occupation numbers of the oxygen sites in the cages, knowing Z cage contained 2 oxygen sites, EZ cage 3 and W cage 4 and accounting for the multiplicity of OZ, OEZ and OW the percentage of cages with respective decoration was derived and compared to the quantitative results of 1D ^{23}Na NMR. The excellent agreement between these methods served as final test to confirm the validity of the used approach and structural models.

1.4. NMR measurements

NMR measurements were performed in a Bruker 500 MHz spectrometer (Avance III; 11.7 T) equipped with a 4mm H/X/Y triple resonance magic angle spinning (MAS) solid-state probe. Larmor frequencies of 1H and 23Na were respectively 500.87 MHz and 132.49 MHz respectively. Sample was filled in a 4mm ZrO_2 rotor and subjected to MAS at 10 / 15 kHz. All ^{1}H and ^{23}Na measurements were acquired with 15kHz MAS. ^{1}H direct excitation spectra were recorded with a π/2 pulse of 83 kHz RF, relaxation delay of 5s and 8 transients. Spectra were recorded at different temperatures from 193K to 333K at intervals of 20K and 253K was selected as the temperature for performing detailed NMR investigations on 1H and 23Na nuclei. ^{1}H Hahn-echo[4] spectrum was acquired with a radio frequency (RF) pulse of 83 kHz, an echo delay equivalent to 3 rotor cycles (200 µs), relaxation delay of 5s and 32 transients. ^{1}H/^{23}Na TRAPDOR measurement was performed with a radio frequency (RF) pulse of 83 kHz on ^{1}H, an echo delay equivalent to 3 rotor cycles (200 µs) during which continuous wave irradiation was performed on ^{23}Na (77kHz RF),

relaxation delay of 5s and 32 transients. ^{1}H-^{1}H 2D exchange spectroscopy (EXSY)[5] was performed with a mixing time of 20 ms, 400 t_e increments of 33.33 µs and 16 transients in the direct dimension. ^{1}H-^{1}H double-quantum – single-quantum (DQ-SQ) spectrum was acquired using the BABA pulse sequence[6] with excitation and conversion periods of 66.67 µs, 400 t_e increments of 33.33 µs and 16 transients in direct dimension. ^{1}H decoupled ^{23}Na spectrum was acquired with a π/12 pulse of 111 kHz RF pulse (solid CT), relaxation delay of 2s, 1024 transients and 1H spinal-64[6] decoupling (50 kHz RF) during acquisition. ^{23}Na triple-quantum (3Q) MAS NMR experiments were performed with the standard three pulse *z*-filtered pulse program. 100 slices were acquired with an increment of 66.67 µs and 144 transients for the direct dimension. ^{1}H-^{23}Na cross polarization – hetcor (cp-hetcor) spectrum was acquired with a recycle delay of 5 s, 0.5 ms cp-contact time, and ^{1}H SPINAL-64[7] decoupling (50 kHz RF) during acquisition. The two dimensional spectrum was acquired with 120 increments of 66.67 µs and 480 transients in the direct dimension. ^{1}H-^{29}Si cp-hetcor.was acquired in a Bruker 800 MHz spectrometer (18.8T; Avance Neo) equipped with a 1.9mm H/X/Y triple resonance MAS probe. Larmor frequencies of ^{1}H and ^{29}Si were 801.25 and 159.19 MHz respectively. The samples was filled a 1.9 mm ZrO_2 rotor and spun at 20 kHz. Recycle delay of 6s, cp contact time of 5 ms, 320 transients in the direct dimension and 64 slices in the indirect dimension with an increment of 40 µs were used for the two-dimensional experiment. ^{1}H spectra were referenced to secondary reference adamantane, which was further referenced to primary reference TMS. ^{23}Na spectrum was referenced to 0.1 M NaCl in D_2O solution. ^{29}Si spectra were referenced to secondary reference, Q8M8 which was earlier referenced to primary reference, TMS. Spectral decomposition was performed with DMFIT software[8].

1.5. DFT calculations

Periodic density functional theory (DFT) calculations were carried out using the BAND module in the Amsterdam Modeling Suite 2020[9]. The PBE[10] exchange-correlation functional was used with a TZP (triple-

ζ plus polarization) basis set and large frozen cores. The Brillouin zone was sampled at the Γ point. Geometry optimizations were carried out at the experimental lattice parameters a = b = c = 8.888 Å. Calculations were performed for both Zundel (**Z**) and Extended Zundel (**EZ**) structures. In all calculations, the framework O, Na, Si, and Al atoms were kept fixed at the positions determined from XRD.

The rational barrier for the $H_3O_2^-$ anion in the Z complex was calculated via a climbing image nudged elastic band calculation. The calculated barrier was 7.6 kcal/mol. Only the O and H atoms were allowed to move for this calculation, so the actual barrier is expected to be even lower due to relaxation of the framework and Na atoms. The interchange of polyhedral geometries is visualized in a supplementary movie S2.

Z: The composition was $Na_8[Al_6Si_6O_{24}](H_3O_2)_2$, where $H_3O_2^-$ is a Zundel-like anion. The Zundel O atoms were initially kept fixed at the XRD-determined positions (together with the framework atoms), and only the positions of the Zundel H atoms were allowed to relax. The initial position was asymmetric, with the central H atom displaced towards one of the O atoms. Upon relaxation of the H positions, the central H atom moved to the center in between the O atoms (figure S13a). This was confirmed to be a local minimum by calculating the partial hessian for the relaxed H atoms. In a second **Z** calculation, also the Zundel O atoms were allowed to relax (figure S13b). This increased the O-O distance from 2.36 Å to 2.40 Å, with the H atom perfectly centered in between the O atoms.

EZ: The composition was $Na_8[Al_6Si_6O_{24}](H_3O_2)(H_2OH_3O_2)$, i.e., a water molecule was added inside one of the Na tetrahedra containing the Zundel anions. A few different initial positions for the water molecule, as well as the hydrogen-bonding arrangement within the water-Zundel complex, were used before relaxing the positions of the water-Zundel complex. All optimizations converged to same local minimum, except for rotations around one of the threefold rotation axes. Because the second Na tetrahedron in the unit cell contained a Zundel anion with fixed orientation, the found local minima did not have

exactly the same energy, but differed by less than 1 kcal/mol. One such local minimum found is depicted in figure S16c, in which two water molecules donate hydrogen bonds to a hydroxide ion.

2. Supplementary figures and tables

2.1. Synthesis compositions and obtained crystalline phases

Table S1: Mother liquor molar compositions of synthesized samples. All samples have compositions of type 0.5 SiO_2 : 0.013 Al_2O_3 : x NaOH : y H_2O. Numbers in the sample labels indicate cation hydration value [H_2O/NaOH] and batch alkalinity [Si/NaOH], respectively.

Sample label	SiO_2	Al_2O_3	NaOH	H_2O	Framework
3.75 – 0.5	0.5	0.013	1.00	3.75	GIS
3 – 0.4	0.5	0.013	1.25	3.75	GIS + SOD
5 – 0.5	0.5	0.013	1.00	5.00	GIS
4 – 0.4	0.5	0.013	1.25	5.00	GIS
3 – 0.3	0.5	0.013	1.67	5.00	SOD[d]
7.5 – 0.5	0.5	0.013	1.00	7.50	GIS
5 – 0.4	0.5	0.013	1.25	7.50	GIS
4.5 – 0.3	0.5	0.013	1.67	7.50	GIS + SOD
3 – 0.2 [a]	0.5	0.013	2.50	7.50	SOD
15 – 0.5	0.5	0.013	1.00	15.00	Amorphous
12 – 0.4	0.5	0.013	1.25	15.00	GIS
9 – 0.3	0.5	0.013	1.67	15.00	GIS + FAU
6 – 0.2	0.5	0.013	2.50	15.00	GIS + SOD
3 – 0.1	0.5	0.013	5.00	15.00	SOD
4.5 – 0.2 [b]	0.5	0.013	2.50	11.25	SOD
5 – 0.1	0.5	0.013	5.00	25.00	SOD
7 – 0.1 [c]	0.5	0.013	5.00	35.00	SOD
10 – 0.1	0.5	0.013	5.00	50.00	GIS + SOD + FAU

[a,b,c] main text samples A, B and C
[d] contains GIS impurity

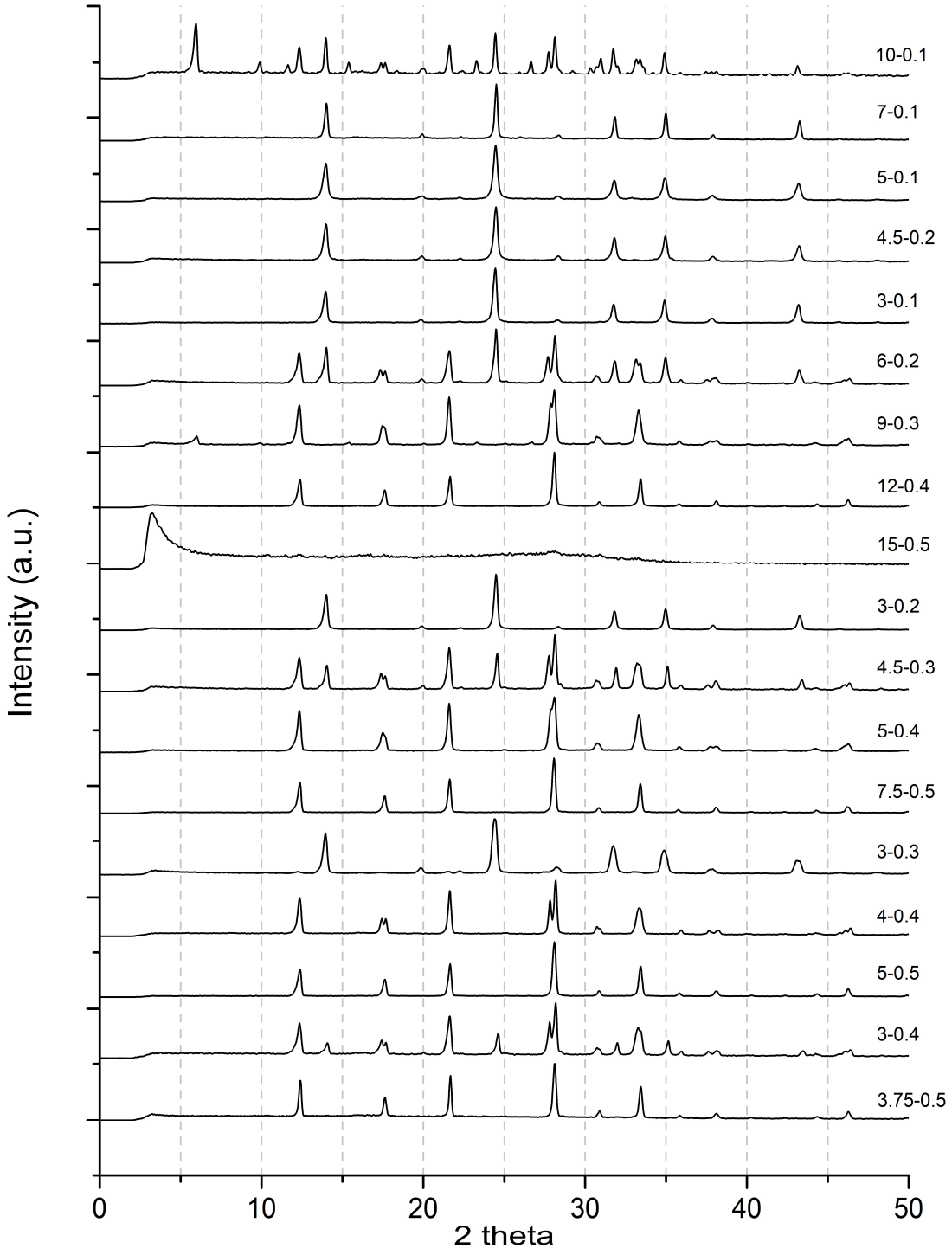

Figure S1: High-throughput diffraction patterns of all samples. Synthesis compositions and formed frameworks of all samples are listed in ESI table 1.

2.2. Refined XRD patterns and parameters

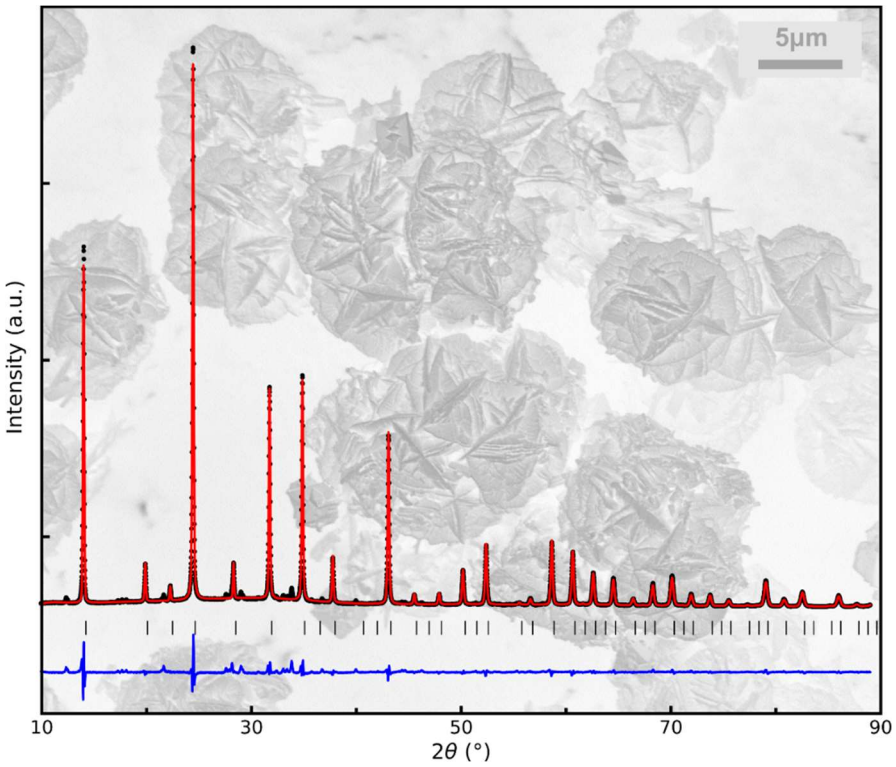

Figure S2: Rietveld refinement plot and SEM image (background) of sample SOD 7-0.1; CSD 2094422

Table S2: Fractional atomic coordinates and isotropic or equivalent isotropic displacement parameters (Å^2) of SOD 7-0.1.

	X	*Y*	*z*	U_{iso}*/U_{eq}	*Occ. (<1)*
Si1	0.0	0.5	0.25	0.00864	
Al2	0.0	0.25	0.5	0.01386	
O1	0.05714 (4)	0.63709 (2)	0.34800 (3)	0.01891	
Na1	0.1699 (3)	0.1699 (3)	0.1699 (3)	0.0487	0.940 (3)
OZ	−0.05891	−0.06004	−0.12159	0.05 (6)*	0.086 (4)
OEZ	−0.10238	−0.10238	−0.10238	0.05 (6)*	0.162 (3)
OW	−0.12942	−0.12942	−0.12942	0.05 (6)*	0.204 (5)

Atomic displacement parameters (Å^2)

	U^{11}	U^{22}	U^{33}	U^{12}	U^{13}	U^{23}
Si1	0.0098 (6)	0.0098 (6)	0.0062 (5)	0.0	0.0	0.0
Al2	0.0188 (5)	0.0038 (8)	0.0188 (5)	0.0	0.0	0.0
O1	0.0099 (7)	0.0156 (6)	0.0311 (7)	0.0073 (1)	−0.0022 (7)	0.0070 (8)

Cubic, *P*-43*n*
a = 8.89768 (3) Å
V = 704.42 (1) Å^3

R_p = 0.051
R_{wp} = 0.073
R_{exp} = 0.037
$R(F^2)$ = 0.041
$(\Delta/\sigma)_{max}$ = 0.06

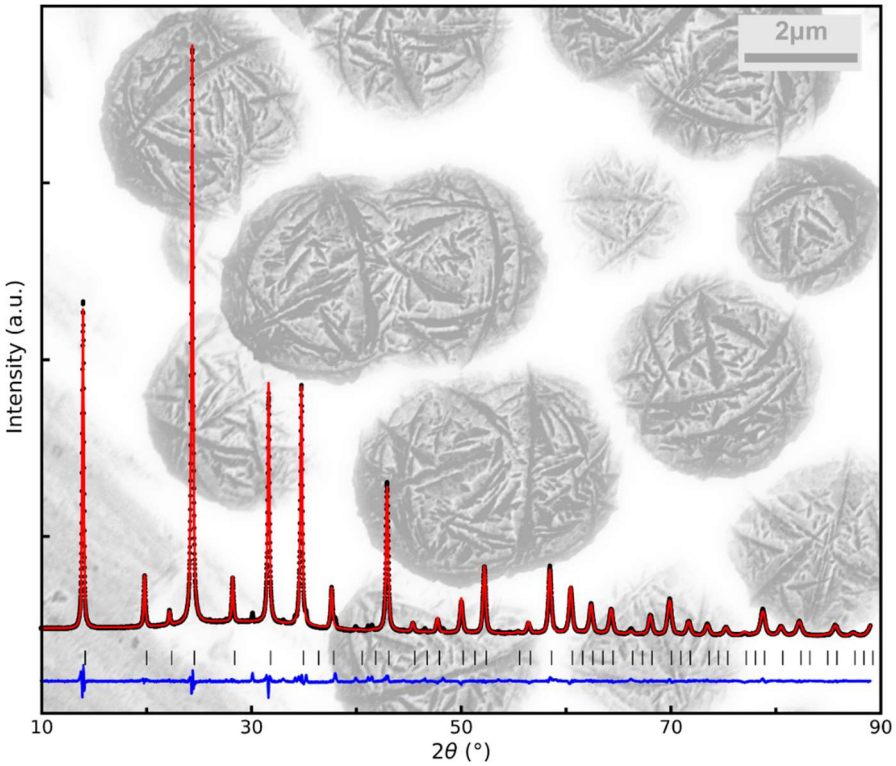

Figure S3: Rietveld refinement plot and SEM image (background) of sample SOD 4.5-0.2; CSD 2094424

Table S3: Fractional atomic coordinates and isotropic or equivalent isotropic displacement parameters (Å^2) of SOD 4.5-0.2.

	X	*y*	*z*	U_{iso}*/U_{eq}	*Occ. (<1)*
Si1	0.0	0.5	0.25	0.01894	
Al2	0.0	0.25	0.5	0.02896	
O1	0.05708 (3)	0.63737 (3)	0.34945 (4)	0.02916	
Na1	0.1694 (8)	0.1694 (8)	0.1694 (8)	0.04025*	0.966 (5)
OZ	−0.05891	−0.06004	−0.12159	0.064 (7)*	0.123 (4)
OEZ	−0.10238	−0.10238	−0.10238	0.064 (7)*	0.103 (3)
OW	−0.12942	−0.12942	−0.12942	0.064 (7)*	0.120 (3)

Atomic displacement parameters (Å^2)

	U^{11}	U^{22}	U^{33}	U^{12}	U^{13}	U^{23}
Si1	0.0216 (6)	0.0216 (6)	0.0135 (7)	0.0	0.0	0.0
Al2	0.0259 (5)	0.0351 (9)	0.0259 (5)	0.0	0.0	0.0
O1	0.0293 (5)	0.0290 (7)	0.0292 (8)	0.005 (9)	0.001 (7)	0.004 (2)

Cubic, *P*-43*n*
a = 8.9288 (6) Å
V = 711.84 (4) Å^3

R_p = 0.045
R_{wp} = 0.063
R_{exp} = 0.031
$R(F^2)$ = 0.066
$(\Delta/\sigma)_{max}$ = 0.07

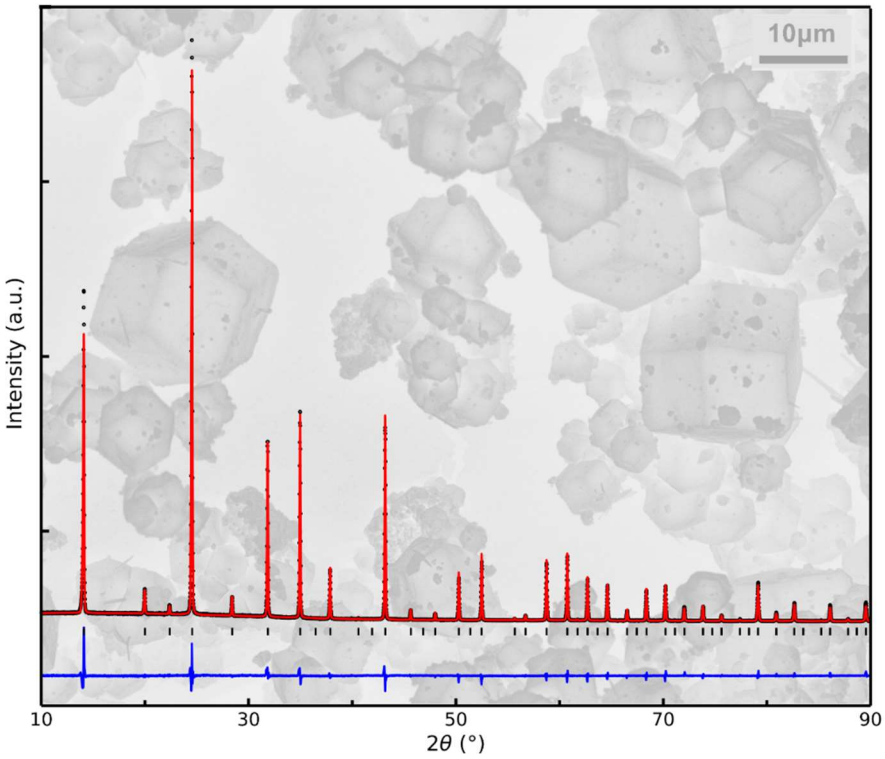

Figure S4: Rietveld refinement plot and SEM image (background) of sample SOD 3-0.2 170°C; CSD 2094423

Table S4: Fractional atomic coordinates and isotropic or equivalent isotropic displacement parameters (Å^2) of SOD 3-0.2 170°C.

	X	*Y*	*z*	U_{iso}*/U_{eq}	*Occ. (<1)*
Si1	0.0	0.5	0.25	0.01733	
Al2	0.0	0.25	0.5	0.01984	
O1	0.05750 (3)	0.63803 (2)	0.34980 (3)	0.02863	
Na1	0.1735 (4)	0.1735 (4)	0.1735 (4)	0.036 (5)*	0.990 (3)
OZ	−0.05891	−0.06004	−0.12159	0.044 (6)*	0.114 (4)
OEZ	−0.1023	−0.1023	−0.1023	0.044 (6)*	0.138 (5)
OW	−0.12942	−0.12942	−0.12942	0.044 (6)*	0.017 (9)

Atomic displacement parameters (Å^2)

	U^{11}	U^{22}	U^{33}	U^{12}	U^{13}	U^{23}
Si1	0.0188 (7)	0.0188 (7)	0.0125 (3)	0.0	0.0	0.0
Al2	0.0244 (4)	0.0142 (5)	0.0244 (4)	0.0	0.0	0.0
O1	0.0236 (6)	0.0313 (4)	0.0310 (4)	0.0017 (8)	0.008 (7)	0.0019 (6)

Cubic, *P*-43*n*
a = 8.88477 (1) Å
V = 701.36 (1) Å^3

R_p = 0.048
R_{wp} = 0.065
R_{exp} = 0.031
$R(F^2)$ = 0.037
$(\Delta/\sigma)_{max}$ = 0.03

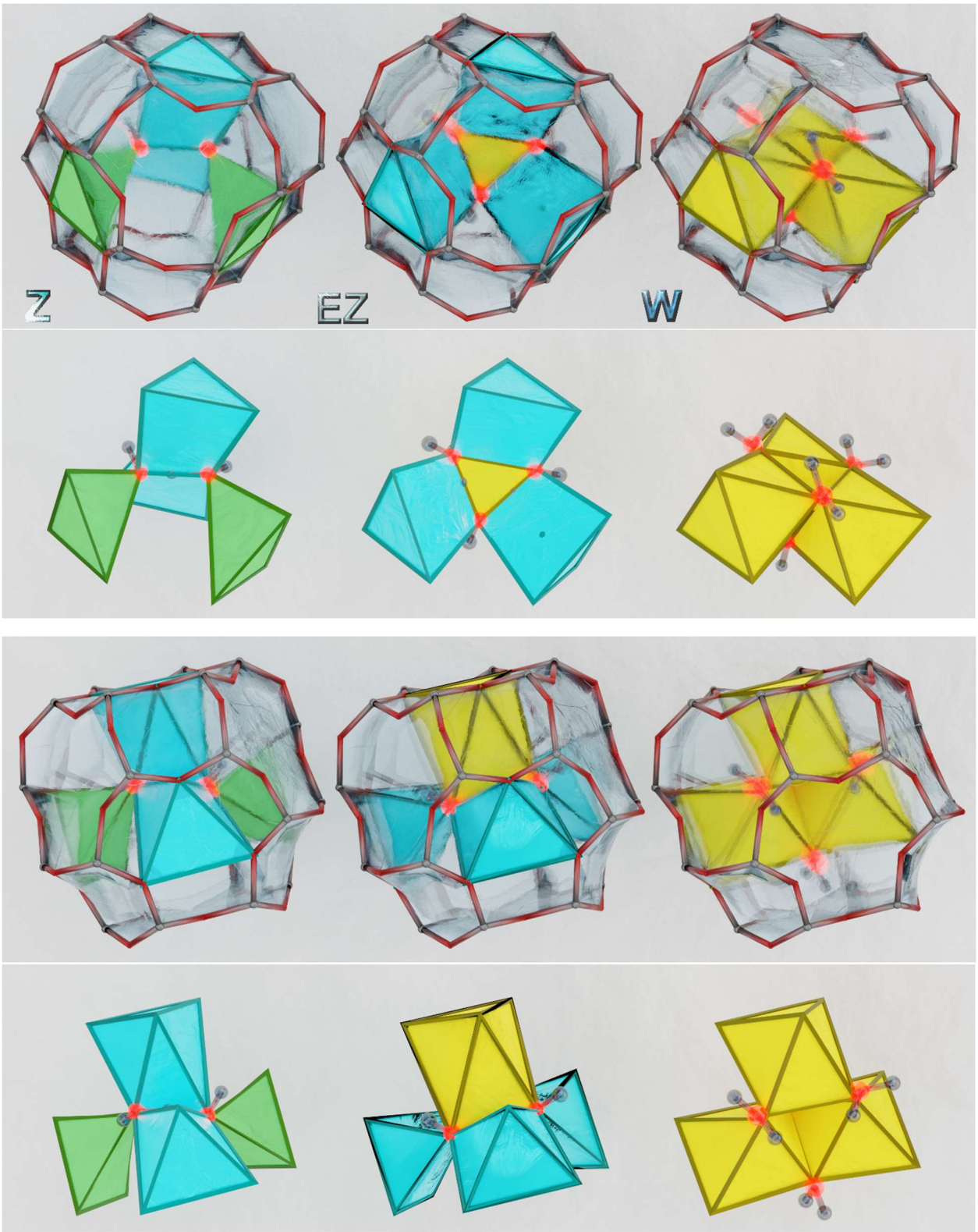

Figure S5*a:* Illustration of coordination polyhedra for the 3 cage decorations Z, EZ and W (from left to right). Shown are two different views. See-saw (green), square pyramid (cyan), and (distorted) octahedral (yellow) polyhedra refer to coordination numbers 4, 5 and 6, respectively. A supplementary movie (ESI movie 1) shows an animation of all three cage decorations.

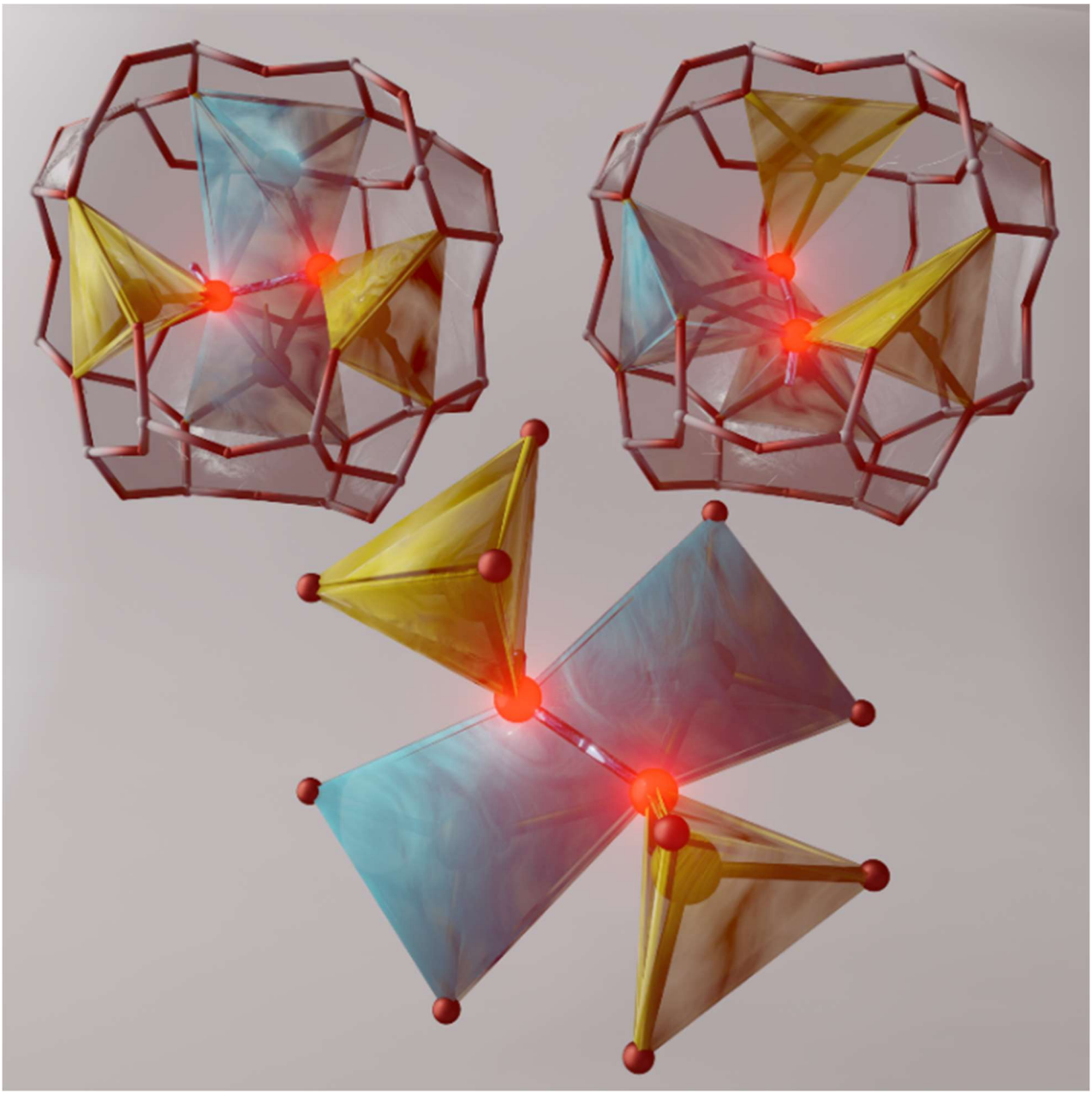

Figure S5*b*: (top) 2 of the 12 possible equivalent configurations of the $H_3O_2^-$ ion in the centre of the sodalite cage. Oxygen atoms of the Zundel anion are in close proximity with strong H-bonding. (bottom). Respective coordination polyhedra resemble see-saw (yellow) and square pyramid (cyan) structures with coordination numbers 4 and 5, respectively. Atomic coordinates were taken from neutron diffraction refinement by Wiebcke et al.[3] A supplementary movie (ESI movie 1) shows and animation of all three cage decorations.

2.3. NMR spectra and decompositions

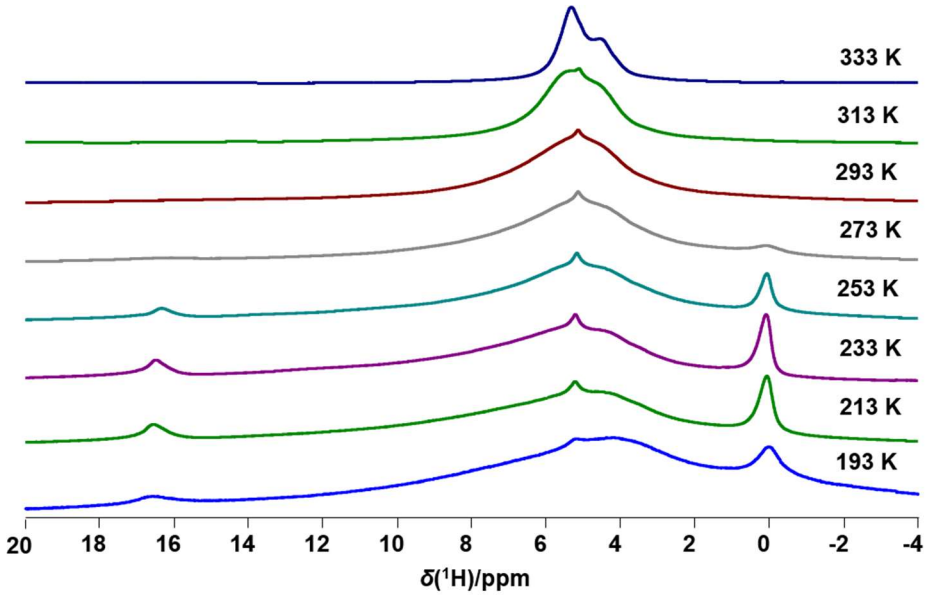

Figure S6: ^{1}H NMR spectra of hydroxysodalite sample B under Variable temperature conditions (193K to 273K) at 11.7T and 15 kHz MAS. All spectra are normalized to height.

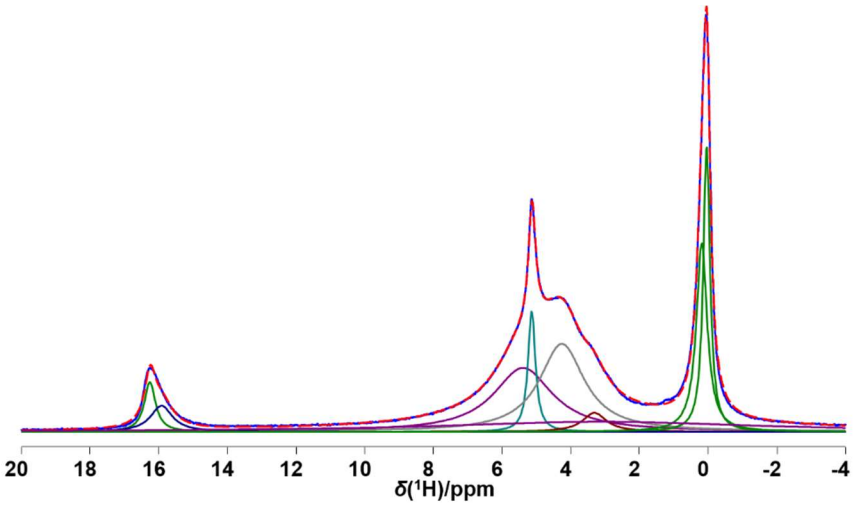

Figure S7: Spectral decomposition of ^{1}H Hahn-echo NMR spectrum of hydroxysodalite sample B (SOD 4.5-0.2) (sample temperature 253K) at 11.7 T.

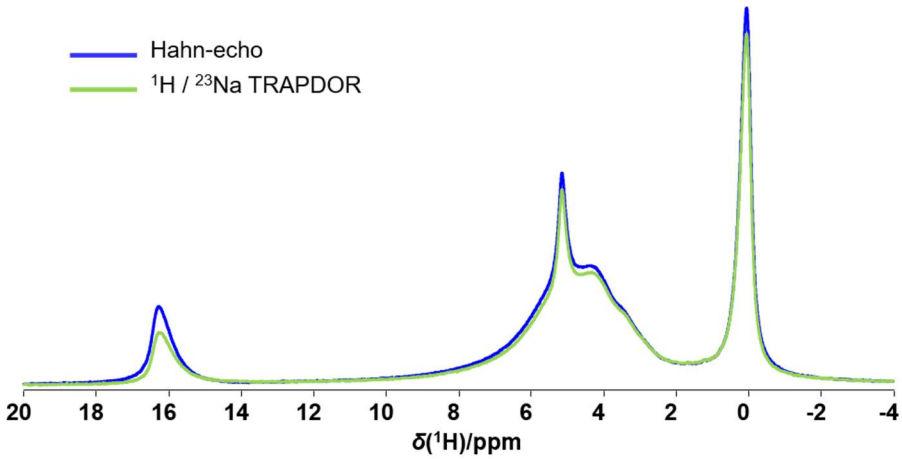

Figure S8:. ^{1}H Hahn-echo (blue trace) and ^{1}H{^{23}Na} TRAPDOR spectrum (green trace) of hydroxysodalite sample B (SOD 4.5-0.2) (sample temperature 253K) at 11.7 T.

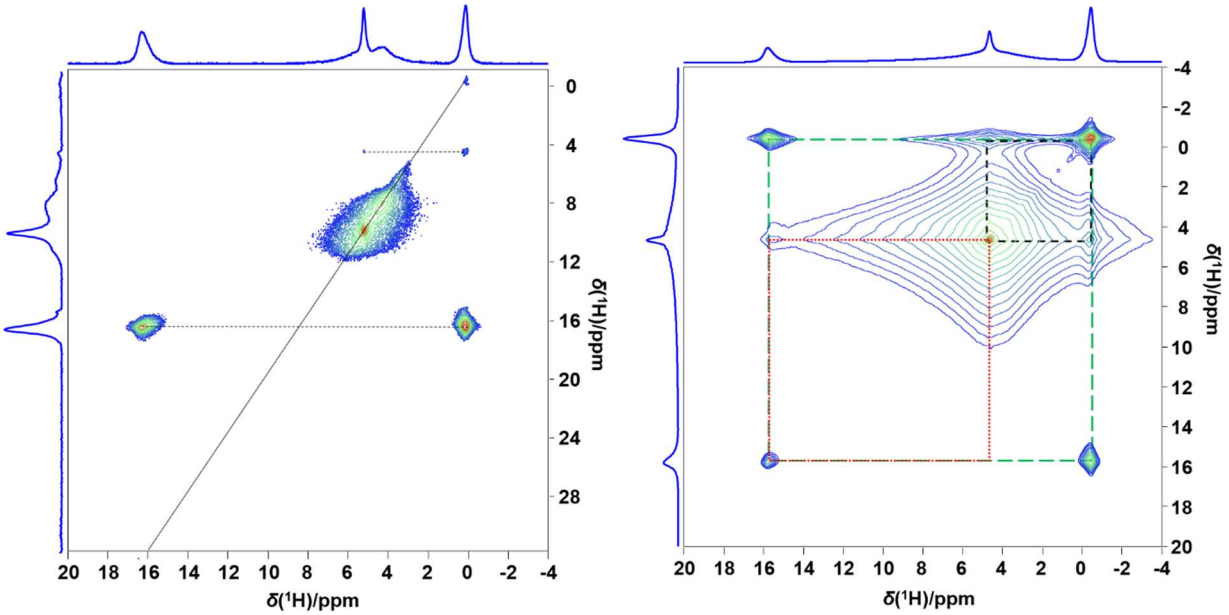

Figure S9: ^{1}H-^{1}H double-quantum – single-quantum (DQ-SQ) (left) and exchange spectroscopy (EXSY) spectrum of hydroxysodalite Sample B (SOD 4.5-0.2) (sample temperature 253K) recorded at 11.7 T.

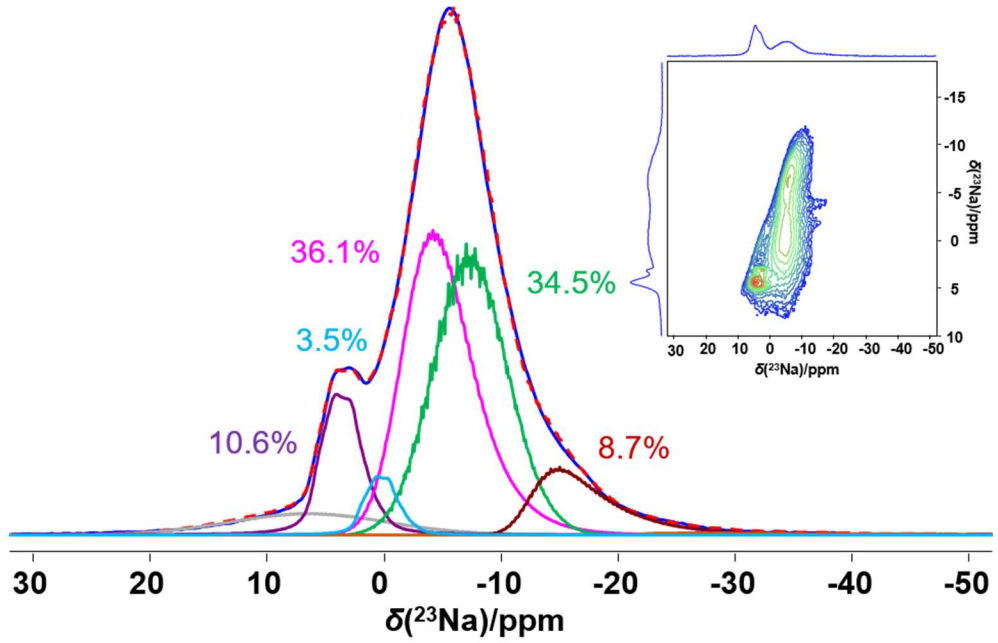

Figure S10: ^{1}H decoupled ^{23}Na NMR spectrum and its spectral decomposition and ^{23}Na 3QMAS spectrum of hydroxysodalite Sample B (SOD 4.5-0.2) (sample temperature 253K) recorded at 11.7 T.

Table S5. Listed are the isotropic chemical shift (δ_{Iso}), quadrupole coupling constant (C_Q), asymmetry parameter (η_Q), relative amounts and assignments of different spectral components in the ^{23}Na direct excitation spectrum of hydroxysodalite Sample B (SOD 4.5-0.2) measured at 11.7 T and 15 kHz MAS.

δ_{Iso}(^{23}Na)/ppm	C_Q (MHz)	η_Q	%	Assignment
7.3	0.7	0.61	5.6	
6.2	1.3	0.49	10.6	EZ-1
2.4	1.2	0.53	3.5	EZ-2
-2.0	1.3	0.61	36.1	Zundel-Middle
-6.0	0.9	0.61	34.5	Zundel-External
-12.3	1.7	0.61	8.7	Water
-21.6	3.1	0.61	0.9	Water

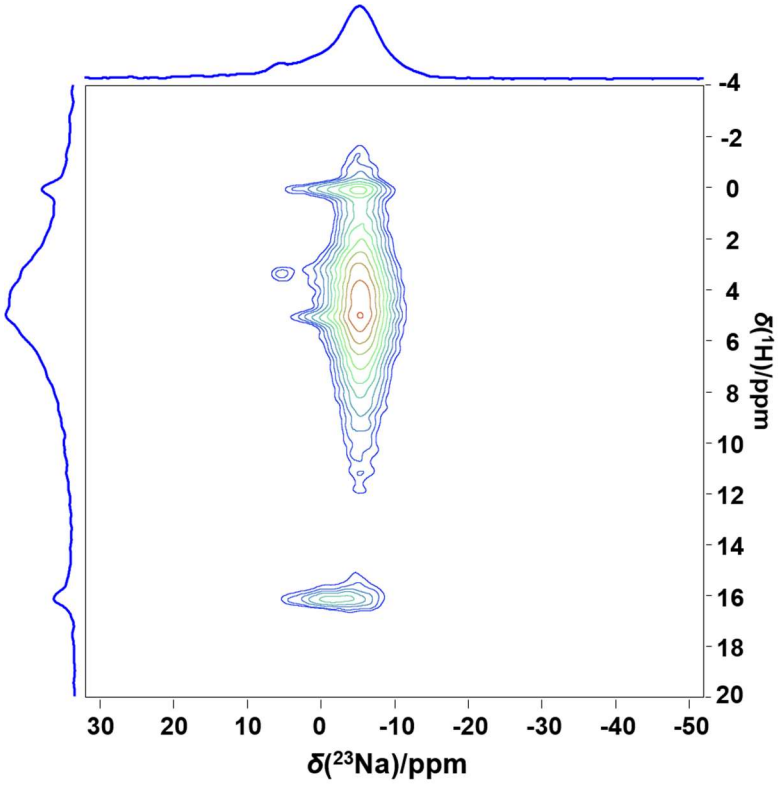

Figure S11: ^{1}H-^{23}Na heteronuclear correlation (HETCOR) NMR spectrum of hydroxysodalite Sample B (SOD 4.5-0.2) (sample temperature 253K) recorded at 11.7 T.

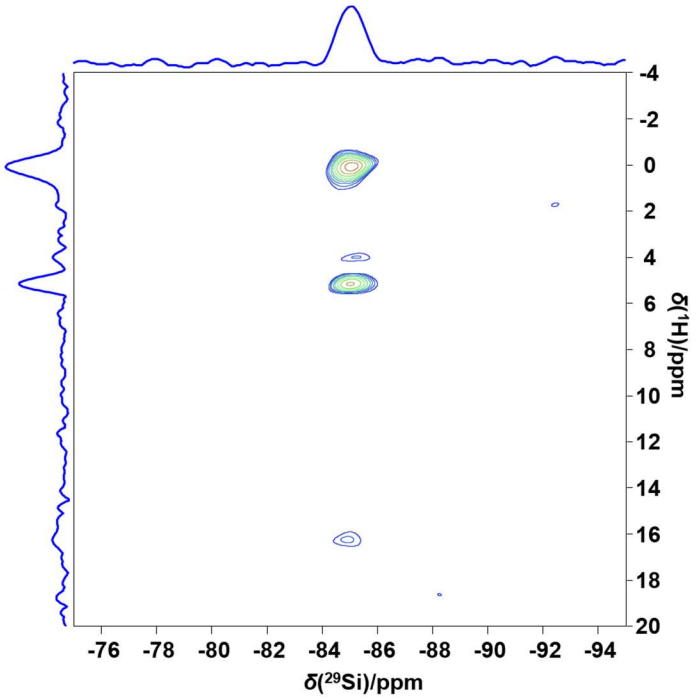

Figure S12: ^{1}H-^{29}Si heteronuclear correlation (HETCOR) NMR spectrum of hydroxysodalite Sample C (SOD 7-0.1) (sample temperature 253K) recorded at 11.7 T.

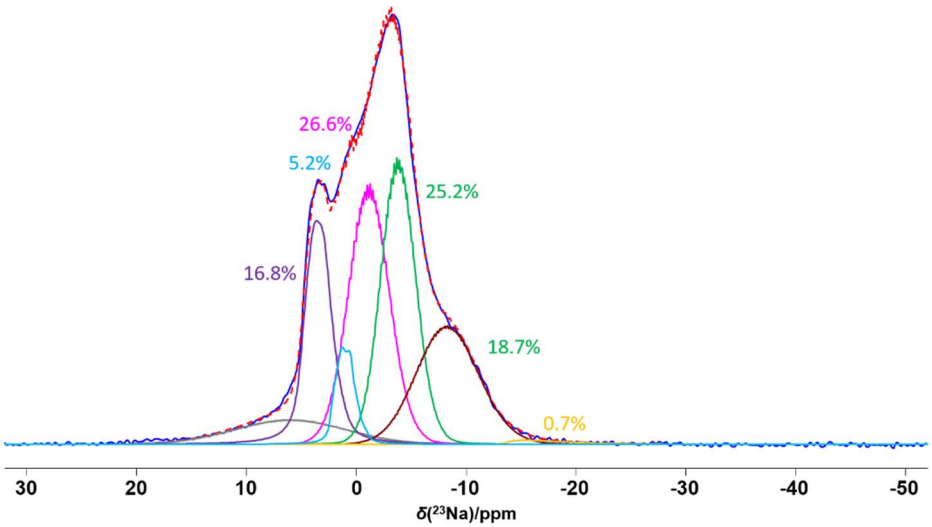

Figure S13: ^{1}H decoupled ^{23}Na NMR spectrum and its spectral decomposition of hydroxysodalite Sample C (SOD 7-0.1) (sample temperature 253K) recorded at 18.8 T.

Table S6. Listed are the isotropic chemical shift (δ_{Iso}), quadrupole coupling constant (C_Q), asymmetry parameter (η_Q), relative amounts and assignments of different spectral components in the ^{23}Na direct excitation spectrum of hydroxysodalite Sample C (SOD 7-0.1) measured at 18.8 T and 20 kHz MAS (sample temperature 253K).

δ_{Iso}(^{23}Na)/ppm	C_Q (MHz)	η_Q	%	Assignment
6.3	0.7	0.61	6.8	
5.1	1.7	0.49	16.8	EZ-1
2.4	1.5	0.49	5.2	EZ-2
-0.7	0.8	0.61	26.6	Zundel-Middle
-3.4	0.8	0.61	25.2	Zundel-External
-7.1	1.4	0.61	18.7	Water
-13.6	2.7	0.61	0.7	Water

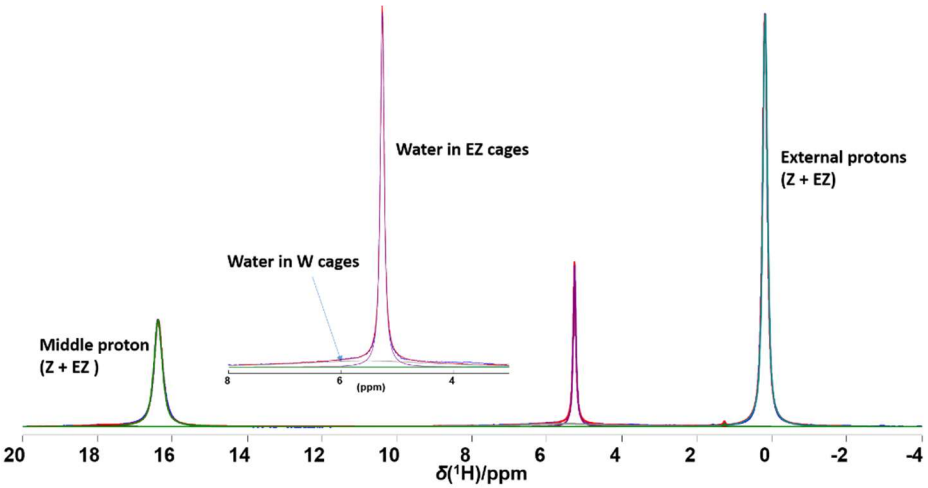

Figure S14: ^{1}H spectrum and its spectral decomposition of hydroxysodalite Sample A (SOD 3-0.2 170°C) (sample temperature 253K) recorded at 11.7 T.

Table S7. Listed are the isotropic chemical shift (δ_{iso}), relative amounts and assignments of different spectral components in the ^{1}H direct excitation spectrum of hydroxysodalite sample A (SOD 3-0.2 170°C) measured at 11.4 T and 15 kHz MAS (sample temperature 253K).

δ_{iso}(^{1}H)/ppm	%	Assignment
17.8	0.83	Z + EZ - middle
16.37	24.67	Z + EZ -middle
5.26	12.3	EZ - H_2O
0.18	53.73	Z + EZ external
5.56	8.3	Water
1.26	0.17	

Table S8. Listed are the isotropic chemical shift (δ_{iso}), relative amounts and assignments of different spectral components in the ^{1}H direct excitation spectrum of hydroxysodalite Sample A (SOD 3-0.2 170°C) measured at 11.4 T and 15 kHz MAS (sample temperature 253K).

	%	Number of ^{1}H in respective architectures	Relative % (corrected to no: of ^{1}H)	% of cages
Zundel-external	41.43			
Zundel-middle	19.35			
Zundel - total	60.78	3	20.26	73.81
EZ-external	12.30			
EZ-middle	6.15			
EZ-H_2O	12.30			
EZ-total	30.75	5	6.15	22.41
W - H_2O	8.30	8	1.04	3.78

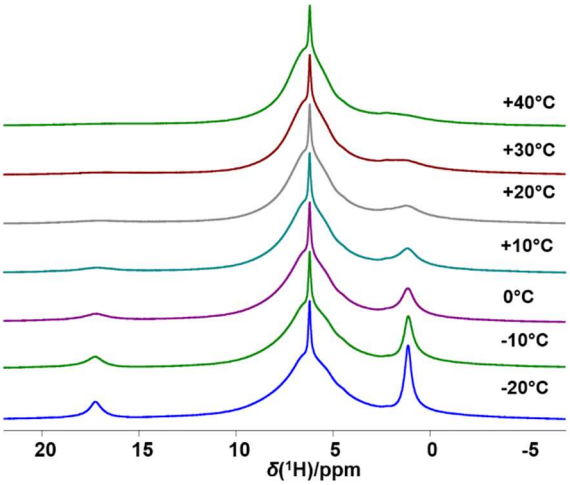

Figure S15: ^{1}H NMR spectra of hydroxysodalite sample C under Variable temperature conditions (253K to 313K) at 18.8T and 20 kHz MAS. All spectra are normalized to height.

2.4. DFT optimized structures

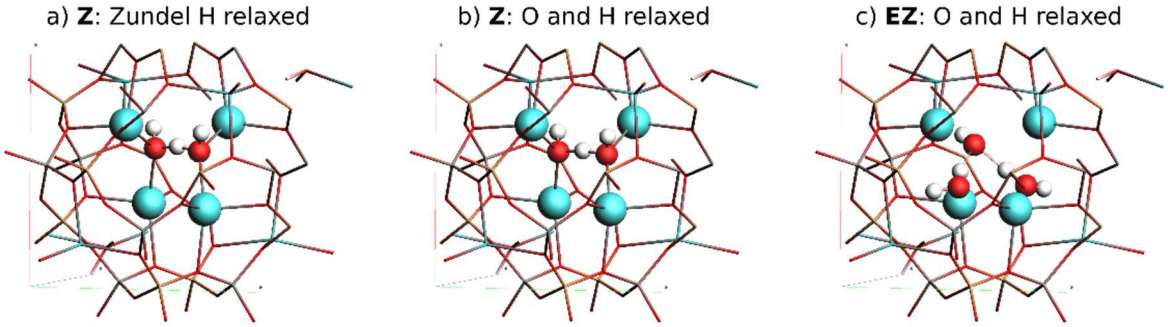

Figure S16: DFT-optimized Zundel structures. a: Structure Z with only H positions relaxed. b: Structure Z with Zundel O and H positions relaxed. c: A local minimum found for structure EZ. The surrounding Na tetrahedra are shown as blue spheres.

2.5. Sodium hydroxide solution coordination chemistry

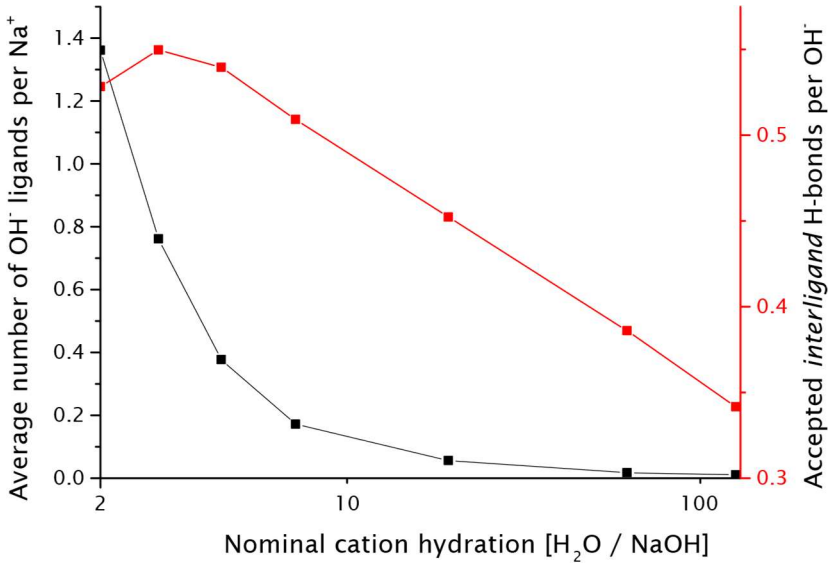

Figure S17: Properties of sodium hydroxide solution chemistry based on simulation by Hellström et al.[12]. The left y-axis shows the average number of OH^- ligands per Na^+ ion. The right y-axis shows the average number of *interligand* H-bonds accepted per OH^- ligand, geometrically implying the existence of Zundel like $H_3O_2^-$ species. Both fractions increase with increased NaOH concentration, here expressed as cation hydration H_2O/NaOH.

2.6. FT-IR

Figure 14 shows the FT-IR spectrum of SOD 3-0.2 170°C, as made (red) and after NaOH extraction with H_2O (blue). The following signal assignments are based on the work of Engelhardt[11], who measured a similar IR spectrum on a pure hydroxysodalite sample ($Na_8[SiAlO_4]_6(OH)_2 \cdot 2H_2O$). The sharp signal at 3640 cm^{-1} is due to the O-H stretching mode of strongly hydrogen bonded H_2O and OH^- species ($H_3O_2^-$) in the sodalite cages. As virtually all water and hydroxide species are part of a Z or EZ complex in the SOD 3-0.2 170°C sample (see section on NMR crystallography), this signal is strong. Furthermore, the typical O-H deformation mode around 1660 cm^{-1} and O-H stretching mode of free water between 4000 – 3000 cm^{-1} is strongly reduced due to the absence of non-hydrogen bonded water in the sodalite cages. After NaOH leaching (ESI section 2.7), resulting in a hydrosodalite phase, water bending and stretching modes are again present by replacement one Na ion and $H_3O_2^-$ with H_2O molecules. Vibrations at wavenumbers below 1200 cm^{-1} are due to Si-O-Al stretching modes of the sodalite framework.

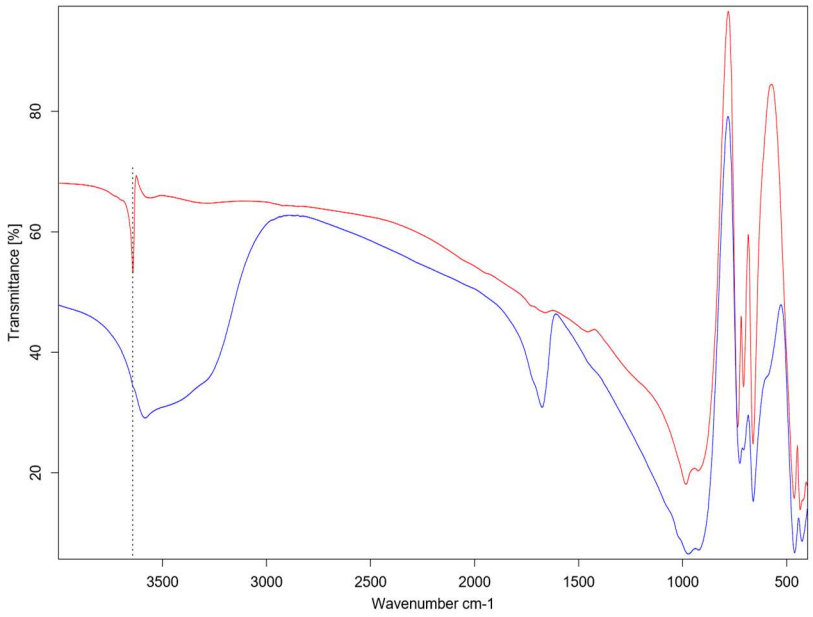

Figure S18*:* FT-IR spectra of SOD 3-0.2 170°C: as-made hydroxysodalite (red) and formed hydrosodalite after NaOH leaching (blue).

2.7. TGA

TGA profile of SOD 3-0.2 170°C (figure 15) shows a weight loss of 6.525% between 60°C and 750°C. Weight loss in hydroxysodalite with general formula $Na_{6+x}[SiAlO_4]_6\ (OH)_x\ .\ yH_2O$ between 500-700°C is due to water leaving the sodalite cages, where 2 OH^- will also form a H_2O molecule, leaving a carnegieite-type phase with interstitial Na_2O[11] (the sodalite framework is destroyed). The chemical composition for this sample predicted by ^{1}H-NMR is $Na_8[SiAlO_4]_6\ (OH)_2\ .\ 2.67\ H_2O$ (as deduced from the relative cage decorations in table 5). The total amount of water molecules leaving the structure as measured by TGA is 3.54 H_2O per unit cell, in good agreement with the predicted value of 3.67. The DTGA profile shows the dehydration occurs in 5 or more discrete steps, exemplifying the variation in cage decoration with Zundel (Z) and extended Zundel (EZ) cages.

Figure 17 shows the TGA profile of the same sample after NaOH removal (hydrosodalite) between 60°C and 750°C. Approximately 11 wt% is lost between 150°C and 300°C due to water leaving the hydrosodalite cages. The small weight loss of approximately 1% between 300°C and 750°C is due to $H_3O_2^-$ decomposition from the cages of the residual hydroxysodalite fraction (see section XX). For pure hydrosodalite with stoichiometry $(NaSiAlO_4)_6\ .\ 8\ H_2O$ a weight loss of 15.7wt% is expected. This indicates the sodalite cages have not yet taken up the maximum amount of water.

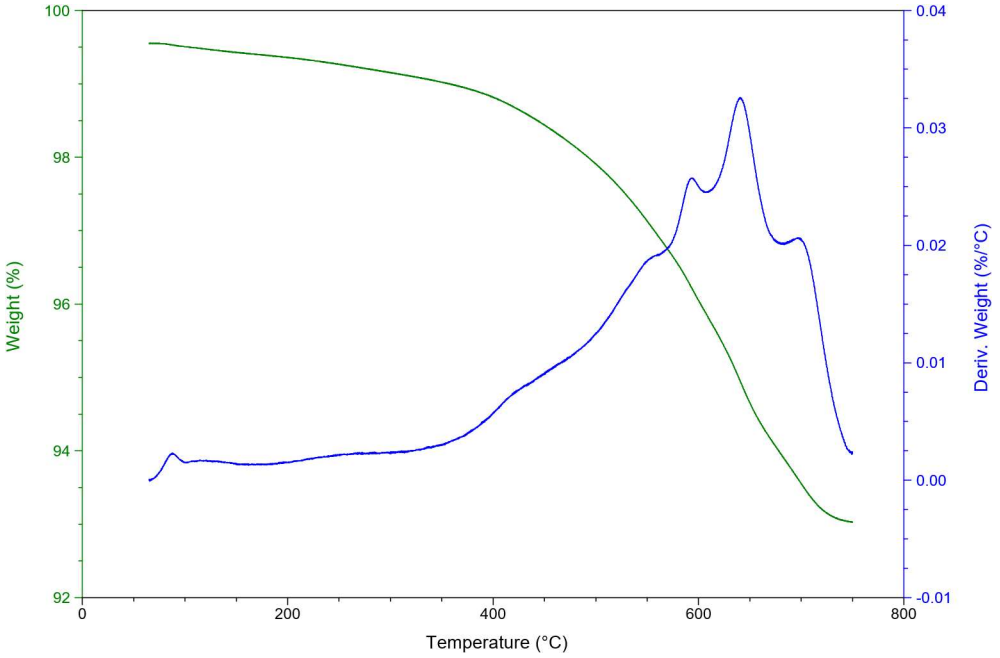

Figure S19: TGA profile and derivative with temperature of sample SOD 3-0.2 170°C (hydroxysodalite).

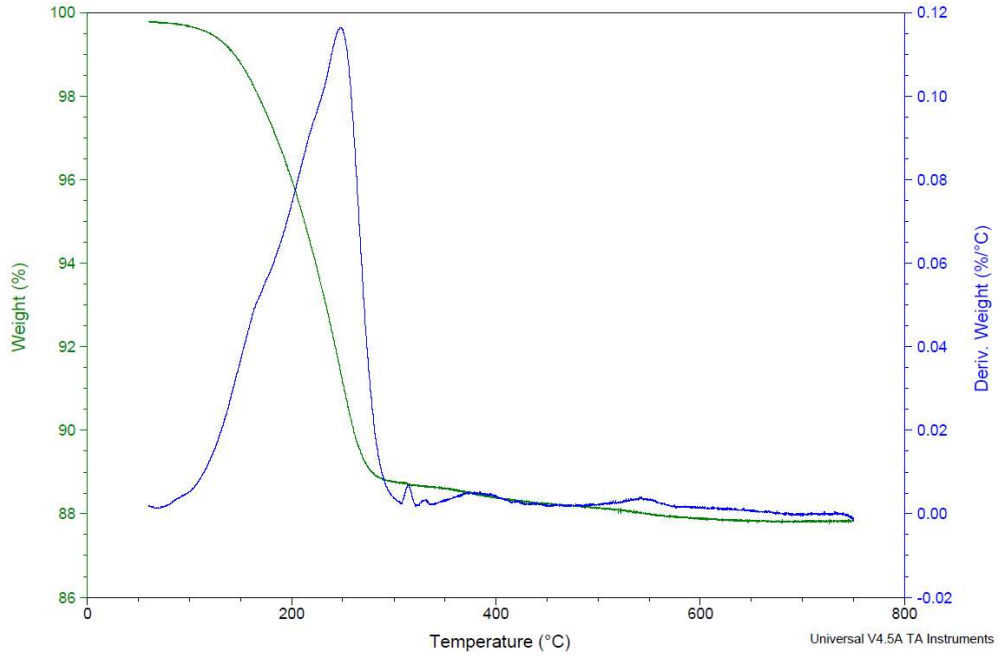

Figure S20: TGA profile and derivative with temperature of sample SOD 3-0.2 170°C after NaOH by leaching (hydrosodalite).

2.8. NaOH leaching experiment

To evaluate the effect on post-synthetic exposure to water, sample A was immersed in deionized water at room temperature and stirred vigorously at room temperature for 7 days. Hydrosodalite $Na_6(SiAlO_4)_6 .8H_2O$ resulting from NaOH extraction due to washing can be readily distinguished by the change of lattice constant, which decreases to 8.848 Å as compared to 8.888Å for ideal hydroxysodalite $Na_8(SiAlO_4)_6.(H_3O_2^-)_2$. This results in a shift of reflections to higher angles. After 7 days at room temperature, the presence of hydrosodalite is evidenced by a shoulder on the hydroxysodalite reflections (ESI fig 18). This shows firstly that prolonged exposure to water at room temperature leads to NaOH extraction, but also that this process is very slow as most of the remaining sample is hydroxysodalite. Second, the observation of peak splitting indicates 2 phases present next to each other, rather than homogeneous solid solutions of different cage decorations in the same crystal. Extraction of NaOH first occurs on the outer layers of the crystals resulting in core-shell like particles where the original hydroxysodalite constitutes the core and hydrosodalite the shell. This zoning of the different phases in the crystals is responsible for the observed peak splitting. This is fundamentally different from the description of the variation in cage decorations of the hydroxysodalite samples in this study, which exist as solid solutions with a statistical distribution of the various cages, depending on the synthesis conditions. The diffraction patterns of these solid solutions do not show peak splitting as there is no zoning of various cage decorations with different lattice constants in the crystals.

To speed up the exchange process the temperature was elevated to 60°C. After 3 more weeks at elevated temperature the sample almost completely transformed to hydrosodalite (ESI fig. 19). The shoulder on the left side of the hydrosodalite reflections shows that a small fraction of non-exchanged hydroxysodalite persists even after this length treatment.

Next, we evaluated whether hydrosodalite could be reconverted to hydroxysodalite by immersion in an excess of concentrated NaOH solution ($[H_2O]/[NaOH] = 3$, mole fraction $n(NaOH) = 0.25$), i.e. the same

NaOH content as used during synthesis of sample A. After two weeks, the solids were recovered by filtration. Based on the mass of the recovered solids, approximately 60% of hydrosodalite had dissolved in the concentrated NaOH solution, showing hydrosodalite is quite soluble under these conditions. The remaining solids were identified as hydrosodalite and there was no indication of reconversion to hydroxysodalite.

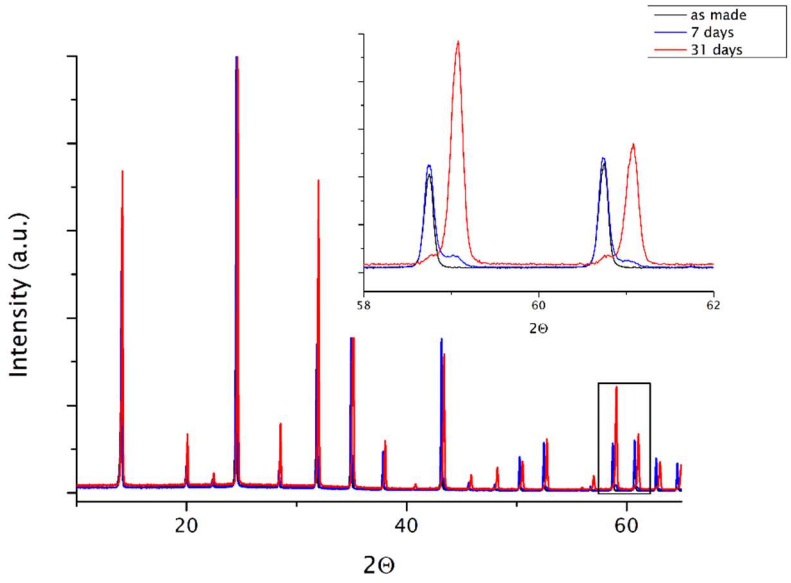

Figure S21: PXRD patterns of hydroxysodalite SOD 3-0.2 170°C, as made (black), after 7 days in H_2O at RT (blue), after 21 more days in water at 60°C (hydrosodalite, red).

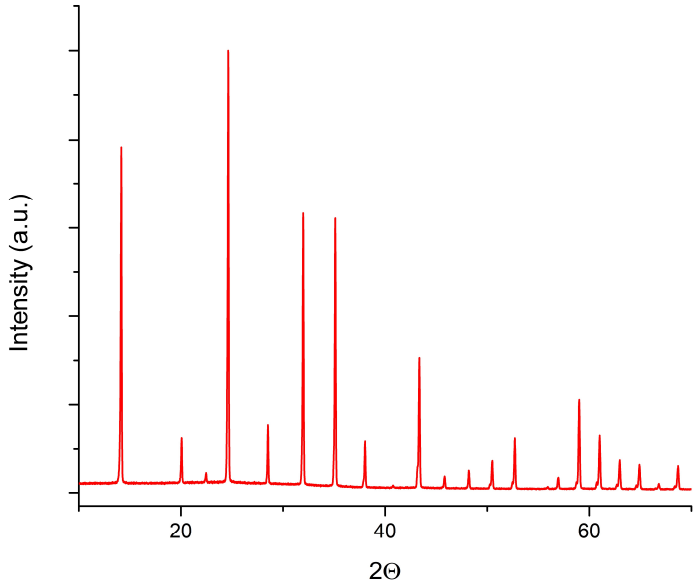

Figure S22: PXRD pattern of hydrosodalite, after re-immersion in concentrated NaOH solution for 14 days.

3. References

1. L. Van Tendeloo, M. Haouas, J.A. Martens, C.E.A. Kirschhock, E. Breynaert and F. Taulelle, *Faraday Discuss*., 2015, 179, 437-449.
2. B. H. Toby, *J. Appl. Cryst.,* 2001, 34, 210-2013
3. M. Wiebcke, G. Engelhardt, J. Felsche, P.B. Kempa, P. Sieger and P. Fischer, *J. Phys. Chem*., 1992, 96, 392-397.
4. E.L. Hahn, *Phys. Rev.,* 1950, 80, 580
5. J. Jeener, B. H. Meier, P. Bachmann and R. R. Ernst, *J. Chem. Phys.*, 1979, 71, 4546–4553.
6. M. Feike, D. E. Demco, R. Graf, J. Gottwald, S. Hafner and H. W. Spiess, *J. Magn. Reson., Ser. A*, 1996, 122, 214–221.
7. B. M. Fung, A. K. Khitrin, and Konstantin Ermolaev, *Journal of Magnetic Resonance*, 2000, 142, 97–101
8. G. te Velde and E.J. Baerends, *Phys. Rev.,* 1991, B 44, 7888
9. BAND 2020, SCM, Theoretical Chemistry, Vrije Universiteit, Amsterdam, The Netherlands, http://www.scm.com
10. J. P. Perdew, K. Burke and M. Ernzerhof, *Phys. Rev. Lett.*, 1996, 77, 3865
11. G. Engelhardt, J. Felsche and P. Sieger, *J. Am. Chem. Soc.,* 1992, 114, 1173-1182
12. M. Hellström, J. Behler, *Phys. Chem. Chem. Phys*, 2017, 19(1), 82-96